Order−Disorder Transition in Surface-Induced Nanopattern of Diblock Copolymer Films

Joachim P. Spatz, Peter Eibeck, Stefan Mössmer, and Martin Möller*

Universität Ulm, Organische Chemie III-Makromolekulare Chemie, D-89069 Ulm, Germany

Elena Yu. Kramarenko, Pavel. G. Khalatur,† Igor I. Potemkin, and Alexei R. Khokhlov

Physics Department, Moscow State University, Moscow 117234 Russia

Roland G. Winkler and Peter Reineker

Universität Ulm, Abt. Theoretische Physik, D-89069 Ulm, Germany

Received May 14, 1999

ABSTRACT: Formation of surface-induced nanopattern (SINPAT) in ultrathin diblock copolymer films is studied by scanning force microscopy and Monte Carlo simulation. The pattern is caused by strong adsorption of one of the two blocks forming a quasi-two-dimensional coil while the other block dewets this adsorption layer. Scanning force microscopy allowed to observe an order−disorder transition for a SINPAT film of polystyrene-*block*-poly(2-vinylpyridine) on mica when the length of the dewetting polystyrene block was varied. The experimental data are compared with the Monte Carlo simulations which demonstrate how the pattern formation depends on the degree of polymerization of the dewetting block and the unfavorable interaction potential between the different components.

Introduction

In bulk, A−B diblock copolymers organize in microdomains if the gain in enthalpy by reducing the contacts between A and B segments exceeds the penalty in entropy by (i) demixing of the A and B segments and (ii) by stretching the chains at the phase boundary.[1] Upon phase separation, the linkages between the blocks get arranged along the borderline of the phases, and a brush-type structure is formed. Steric crowding causes some stretching of the chains, resulting in a repulsive elastic contribution to the free energy. The phase state can be correlated with the product of the Flory parameter χ_{A-B} and the number of monomer units N; i.e., the order−disorder transition depends on $\chi_{A-B}N$. For small values of the product $\chi_{A-B}N < 10$ (weak segregation regime), the blocks mix and the chain conformation is Gaussian. For $\chi_{A-B}N \gg 10$ (strong segregation limit) nearly pure microdomains are formed separated by narrow interfaces.[2,3] The shape and size of the microdomain structure in the strong segregation limit are primarily controlled by the volume fraction of the constituent blocks.

The proximity of a macroscopic phase boundary can affect the orientation of the microdomains as well as their structure. Parallel orientation of lamellae to the substrate is observed in thin films of a symmetrical polystyrene-*block*-poly(methyl methacrylate) on a SiO_2 surface.[4] The phase morphology of a diblock copolymer is also strongly affected by the confinement between two walls and the chemical composition of the walls, i.e., the interfacial energies.[5,6] In the case of a lamellae structure, the lamellae get compressed or thicken in order to satisfy the geometric constraints. If the mismatch of the periodicity and the film thickness is too large, cylinders or lamellae are formed that are oriented perpendicular to the surface. Also, electric fields can have strong influence on the orientation of diblock copolymer domains.[7] In general, there is a strong tendency that the interface or surface is covered by a thin, chemically uniform layer of the block copolymer component that yields the lowest interfacial energy.[8−11]

Scheme 1

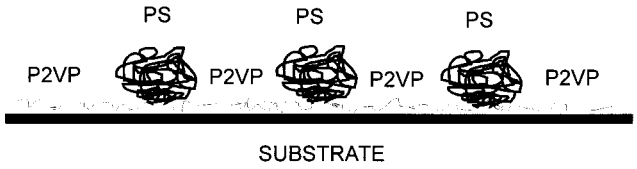

As reported recently, ultrathin films of a polystyrene-*block*-poly(2-vinylpyridine) diblock copolymer (PS-*b*-P2VP) on mica can form a chemically heterogeneous surface pattern.[12−16] To achieve this, the films have to be prepared in such a way that the average thickness of the polymer is much less than the equilibrium period of the bulk morphology. In this case, the strongly adsorbed P2VP blocks wet the mica surface as an ultrathin, approximately 1 nm thick polymer layer whereby the chain formation gets largely extended. The PS blocks dewet the P2VP layer and aggregate to surface clusters in order to minimize the number of unfavorable contacts with the polar blocks and the air. The structure of these surface-induced nanopatterns (SINPAT) is schematically shown in Scheme 1. Similar surface micelle structures were observed with a diblock copolymer with one hydrophobic block and one polyelectrolyte block that adsorbed at the air−water interface.[17,18]

In a scaling analysis, it was shown that the number of chains in one surface micelle as well as the radius

* To whom correspondence should be sent.
† Present address: Department of Physical Chemistry, Tver State University, Tver 170002, Russia.

10.1021/ma990751p CCC: $19.00
Published on Web 12/10/1999

Table 1. Molecular Weights and Block Lengths of the Synthesized Block Copolymers

	PS		block		P2VP	
polymer[a] PS(x)-*b*-P2VP(y)	M_n[b] [g/mol]	M_w/M_n[b]	M_n[c] [g/mol]	M_w/M_n[c]	DP[d] (^{1}H NMR)	DP[e] (EA)
80-330	8300	1.06	57 600	1.10	332	
190-320	19400	1.05	62 300	1.11	320	
230-270	24400	1.04	60 100	1.10	270	
300-300			60 000	1.10	300	300
1350-400	140800	1.11	182 300	1.11	395	402

[a] x and y give the numbers of repeating units according to the monomer/initiator ratio. [b]Molecular weight of the first block, obtained from SEC in THF with narrow distributed poly(styrene) standards. [c] Molecular weight of the block copolymer, obtained from SEC in DMA with narrow distributed poly(styrene) standards. [d] Block length of poly(2-vinylpyridine), calculated from the styrene/2-vinylpyridine composition obtained by ^{1}H NMR in relation to the PS block. [e] Block length of poly(2-vinylpyridine), derived from elemental analysis.

and the height of the micelles will depend on the length N_B of the nonadsorbed blocks as $N_B^{1/2}$; this means that the conformation of B blocks in the surface aggregates is nearly Gaussian. The distance between neighboring associates scales as $D \sim N_A^{1/2} N_B^{1/4}$.[15] Depending on the block length ratio and the interaction parameters, the dewetting B blocks can assemble either into globular surface micelles or into wormlike surface associates; i.e., a point or a striped surface pattern is formed.[16]

In this report, we focus on the question of how the order of the SINPAT depends on the molecular weight of the dewetting PS blocks and the substrate on which the film is cast.

Experimental Section

Materials. Chloroform (Merck, p.A.) was used as received. Mica plates (muscovit) were received from BAL-TEC ($P = 10$, BU 006 027-T) and freshly cleaved prior to use. The GaAs wafer (grown by Molecular Beam Epitaxy at the Abt. Halbleiterphysik, Universität Ulm, K. Bizer) was cleaned in an ultrasonic bath in acetone (p.A.) for 2 h.

Polymerization. Block copolymers of poly(styrene)-*block*-poly(2-vinylpyridine) (PS-*b*-P2VP) with different molecular weights were synthesized by means of living, anionic polymerization (see Table 1). The prepurified monomers have been dried on a high-vacuum line by three subsequential freezing−evacuation−melting cycles and distilled under high vacuum into ampules, equipped with PTFE valves, following standard techniques.[19,20] After termination with methanol and precipitation in petrol ether, the polymers were characterized by means of SEC, NMR, and elemental analysis.

Sample Preparation. For the preparation of the SINPAT films, 0.01 mg/mL of the corresponding diblock copolymer was dissolved in chloroform. In dilute solution of chloroform, light scattering experiments showed no association of the PS-*b*-P2VP block copolymers. The very dilute solutions were spun-cast onto a freshly cleaved piece of mica or a clean GaAs wafer with a rotation speed of 10.000 rpm. Alternatively, the substrates were dipped into the solution and pulled out with a constant velocity of 10 mm/min. The polymer films were annealed at 150 °C for 48 h under vacuum.

Scanning Force Microscopy. The surface topology and sample thickness were investigated by means of scanning force microscopy (SFM) using a Nanoscope III working in the tapping or contact mode at ambient conditions. The sample thickness was determined by removing the polymer from the substrate using high tip forces during scanning in contact mode. Usually, an area of 500 × 500 nm^2 of the plain substrate was exposed which allowed to determine the sample thickness.[12]

Evaluation of Sample Parameters and Error Estimations. SINPATs were evaluated for the mean cluster to cluster distance, P, the mean cluster height, h, the number of clusters per unit area, #, and the mean cluster radius, r. The mean cluster to cluster distance, P, was determined to be equal to the reciprocal value of the maximum intensity position of the Fourier transformation of a 5 × 5 μm^2 SFM image. The Fourier transformation was performed using the Nanoscope III software 4.2. The error of P, ΔP, was estimated by the half-intensity width of the maximum distribution of the Fourier transform. An average of 20 single cluster height values obtained from the SFM height images was taken as the mean cluster height, h. The height error, Δh, was estimated from the statistical scattering of the single cluster height values. The number of clusters per unit area, #, was obtained by counting all clusters higher than 2 nm in an area of 1 μm^2 using the Nanoscope III software 4.2. The error Δ# was determined to be the maximum difference between the number of clusters higher than 1 and 3 nm and #. For the evaluation of the mean cluster radius r from the scanning force microscopy images, one has to take into account the convolution with the curvature of the tip apex, t, which causes an systematic error by enlarging the cluster radius in the image by roughly the radius of the tip apex. The apex itself varies by 10% for different tips. Tips were changed for each sample because of contamination. The mean cluster radius, r_0, was determined as the average of 20 single cluster radii with Δr_0 representing the statistical scattering of the single imaged cluster radii. We approximated that all tips had a tip radius of $t = 10$ nm by which the apparent cluster radius, r, is enlarged. This value has been subtracted from the imaged cluster radius values r_0:

$$r = r_0 - t$$

The error in the mean cluster radius was calculated to be

$$\Delta r = \Delta r_0 + \Delta t$$

The number of aggregated PS chains per cluster, Q, was obtained by applying the following formula assuming a cone-like volume of the clusters and $\rho = 1.1$ g/cm^3 for the density of PS:

$$Q = \frac{{}^1/_3 \pi (r_0 - t)^2 h \rho N_L}{M_{PS}}$$

with $r = r_0 - t$, N_L = the Avogadro number, and M_{PS} = the molecular weight of PS. The error of the number of aggregated PS chains was calculated to be

$$\Delta Q = 2Q\left(\frac{\Delta r_0}{r_0} + \frac{\Delta t}{t} + 0.5\,\frac{\Delta h}{h}\right)$$

Results and Discussions

Ultradilute solutions of the diblock copolymers in $CHCl_3$ were spun- or dip-cast on freshly cleaved mica or a purified GaAs wafer. Chloroform was chosen as a solvent because it dissolves both blocks rather well and does not promote the formation of micelles. Thus, the surface structures are formed by adsorption of individual block copolymer molecules. To obtain a surface pattern that corresponds to a minimum in the free energy, all samples were annealed at 150 °C under vacuum for at least several hours, which is significantly above the bulk glass temperature of the two blocks.

Figure 1a−d shows SFM topography images of a series of PS-*b*-P2VP diblock copolymers. The image size corresponds to 1 μm × 1 μm. The gray scale on the top depicts the scale of height variations ranging from 0 nm for black and 20 nm for white surface areas.

Figure 1a shows a rather regular pattern, which has been obtained with the PS(300)-*b*-P2VP(300) diblock

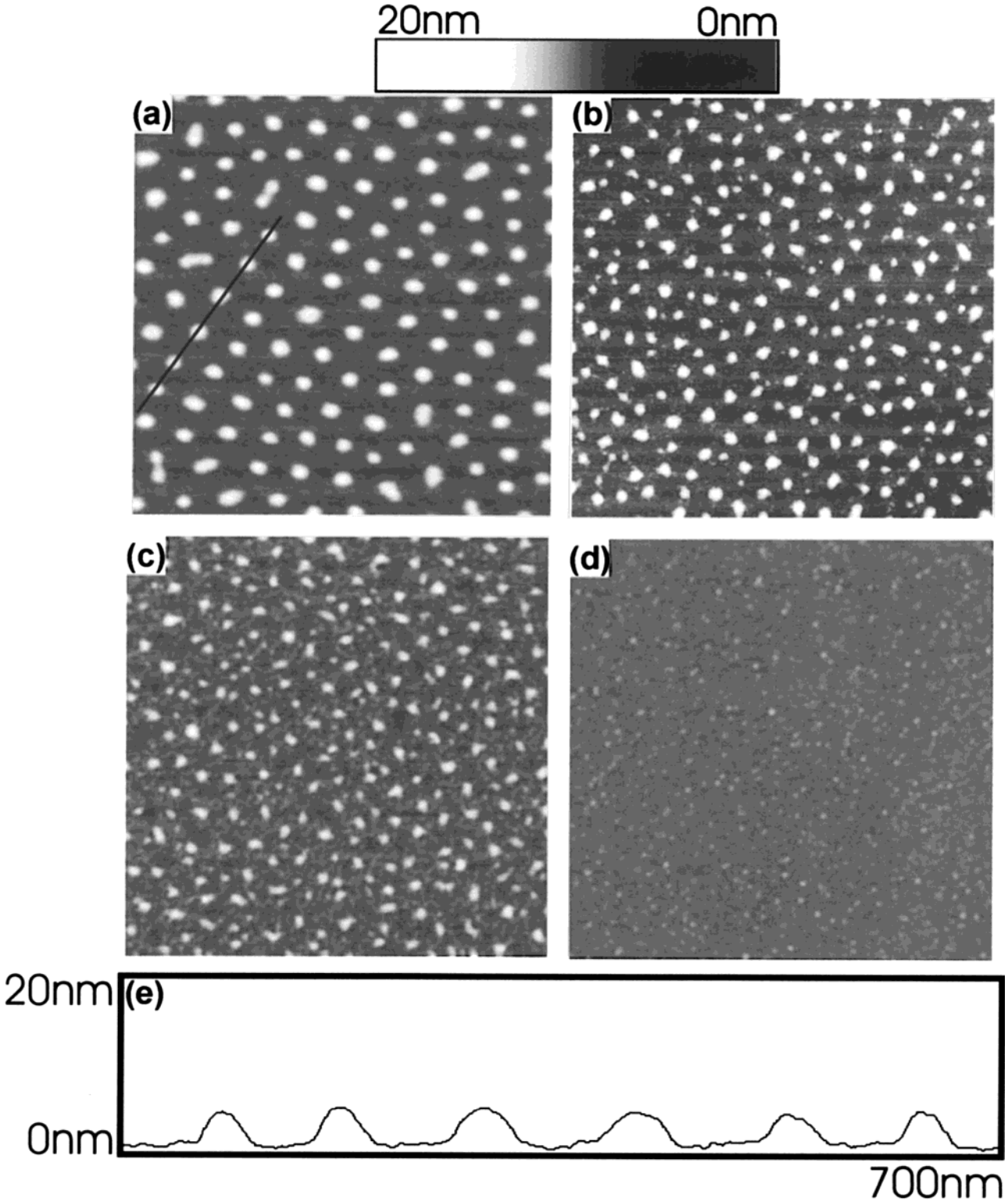

Figure 1. SFM topography images of laterally phase separated diblock copolymer films. The gray scale indicates the height values ranging from 0 nm for black and 20 nm for white features. The width of each image corresponds to 1 μm: (a) PS(300)-*b*-P2VP(300), (b) PS(230)-*b*-P2VP(300), (c) PS(170)-*b*-P2VP(300), and PS(70)-*b*-P2VP(300). (e) Height profile following the horizontal line indicated in (a).

copolymer (see Table 2). The bright spots are uniform in height and surface. As schematically shown above, they represent clusters of agglomerated PS chains.[12] By X-ray photoelectron spectroscopy and detailed SFM investigations, it has been demonstrated that the clusters are separated by only a 1 nm thick layer of P2VP chains that are tightly adsorbed to the mica substrate.[12] The height profile (Figure 1e) has been taken along the black line indicated in Figure 1a. The average cluster to cluster distance is $P = 100 \pm 10$ nm, and the average height is 5 ± 0.5 nm. Counting all clusters per μm^2 yielded the number of clusters per unit area to $\# = 110 \pm 5$ $1/\mu m^2$. The average cluster radius r has been estimated taking into account the convolution of the cluster profile with the curvature of the tip apex. In the case of Figure 1a the cluster radius is $r = 20 \pm 6$ nm.

Table 2. Characteristic Values of Lateral Phase Separated PS(N_{PS})-*b*-P2VP(N_{P2VP}) Diblock Copolymer Films[a]

N_{PS}-*b*-N_{P2VP}	r [nm]	Q	P [nm]	# [μm^{-2}]	h [nm]
80-*b*-330[b]			50 ± 50	410 ± 100	<2
190-*b*-300[b]	10 ± 7	12 ± 12	70 ± 30	280 ± 30	3 ± 1
230-*b*-300[b]	12 ± 6	23 ± 17	75 ± 25	250 ± 20	5 ± 0.5
300-*b*-300[b]	20 ± 6	45 ± 29	100 ± 10	110 ± 5	5 ± 0.5
1350-*b*-400[b]	55 ± 8	164 ± 86	350 ± 40	8 ± 2	11 ± 1
1350-*b*-400[c]	35 ± 7	48 ± 34	220 ± 40	21 ± 3	8 ± 2

[a] r = average cluster diameter, Q = average number of agglomerated chains per single cluster, P = average cluster to cluster distance, # = average number of clusters per unit area, h = average height of the cluster. [b] Onto mica. [c] Onto GaAs wafer.

Assuming a conelike volume of the clusters and $\rho = 1.1$ g/cm^3 for the density of PS, the average number of agglomerated PS chains is calculated to be $Q = 45 \pm 29$ where the large uncertainty in Q appears from the difficulties in the precise determination of the cluster radius.

Figure 1b shows a SINPAT film that has been obtained with a diblock copolymer with a shorter PS-block, PS(230)-*b*-P2VP(300). While the average cluster height did not change significantly, the size and the shape became considerably less uniform, and the clusters decreased in volume. This is indicated by a considerably smaller number of agglomerated PS chains per cluster and a large distribution in the cluster sizes, $Q = 23 \pm 17$ and $r = 12 \pm 6$ nm. The average cluster to cluster distance decreased to $P = 75 \pm 25$ nm. The number of clusters per μm^2 increased to # = 250 ± 20 1/μm^2, and the average cluster height was 5 ± 0.5 nm. The thickness of the P2VP film between the clusters did not change compared to the sample in Figure 1a remaining about 1 nm.

Figure 1c shows the corresponding SINPAT film of a PS(190)-*b*-P2VP(300) diblock copolymer. The average cluster height decreased to $h = 3 \pm 1$ nm, and the dispersity of the cluster size increased further while the average number of PS chains per cluster decreased to $Q = 12 \pm 12$ and the average cluster radius to $r = 10 \pm 7$ nm. The average cluster to cluster distance was determined to $P = 70 \pm 30$ nm, and the number of cluster per unit area increased to # = 280 ± 30 1/μm^2. Again, the thickness of the P2VP film between the clusters was 1 nm.

Figure 1d shows the film formed by a PS(80)-*b*-P2VP(330) diblock copolymer. Clearly, the ability to form a regular pattern was lost as the length of the PS block was decreased to this extend. Only very small and rather irregularly arranged clusters were formed with a height smaller than 2 nm. The number of clusters per unit area increased to # = 410 ± 100. The corresponding average distance decreased to 50 ± 50 nm.

The decrease in order as the length of the PS block is diminished is also demonstrated by the 2D Fourier transformation of the images depicted in Figure 2a−d. The Fourier transformation of the pattern obtained with the PS(300)-*b*-P2VP(300) sample shows a distinct first-order and a weak second-order ring. With decreasing length of the PS block the maximum shifts toward the center, and the ring broadens. Figure 2d does not indicate any order when the length of the PS block was reduced by a factor of 4.

Figure 3a shows a height image of a SINPAT film on mica obtained with a PS(1350)-*b*-P2VP(400) diblock copolymer film prepared by dip-casting and annealed at 150 °C under vacuum for 48 h. The molecular weight of the PS block is by a factor of 4.5 higher than in the case of the PS(300)-*b*-P2VP(300) sample which was used to prepare the film shown in Figure 1a. The length of the P2VP block is about the same. The significant effect of the length of the PS block is evident. The average cluster to cluster distance increased to $P = 350 \pm 40$ nm, the number of agglomerated chains per cluster to a remarkable $Q = 164 \pm 86$, the cluster height to $h = 11 \pm 1$ nm, and the number of clusters per unit area decreased to # = 8 ± 2 1/μm^2.

Also, the choice of the substrate influences the order and the size of the pattern. Figure 3b shows an ultrathin film of the same diblock copolymer as in Figure 3a which, however, has been prepared on a GaAs wafer by dip-coating. Also in this case the film was annealed at 150 °C for 48 h. The clusters are no more uniform in size; the number of agglomerated chains per cluster decreased to $Q = 48 \pm 34$ nm. The cluster height decreased to $h = 8 \pm 2$ nm, the average cluster to cluster distance decreased to $P = 220 \pm 40$ nm, and the number of clusters per unit area increased to # = 21 ± 3 1/μm^2.

In summary, it can be concluded that the molecular weight of the PS block has a significant influence on the order of the SINPAT films as expressed by the uniformity of the cluster volumes and the uniformity of the cluster to cluster distances. As the length of the PS block is increased, also the incompatibility becomes larger between the PS chains and the underlying P2VP/mica interface and the air. As a consequence, unfavorable contacts between styrene units and the P2VP/mica sublayer and the air are reduced by increasing the number of chains per cluster. The gain in enthalpic energy can cause further chain stretching. On the other hand, entropic forces become dominant if the molecular weight of PS is decreased and segregation is less favorable. Furthermore, also the choice of substrate plays a key part in the organization of the SINPAT structures. The observation that a much less ordered pattern was achieved on the GaAs substrate than with mica indicates that the interaction of the PS chains with GaAs is much more favorable than with mica covered with a thin layer of poly(2-vinylpyridine).

Complementary to the SFM experiments, the formation and ordering of the SINPAT films has been studied also by computer simulations employing a Monte Carlo lattice method[21] based on a "bond fluctuation model" which is advantageous in simulation of dense systems.[22]

A cubic simulation box was applied with lattice and periodic boundary conditions in the XY plane with an edge length of $L_x = L_y = L = 128$ (measured in units of spacing b). In the Z direction the system was confined by two planes $Z = 0$ and $Z = Z_0$. The adsorbed blocks (blocks A) were modeled as two-dimensional coils on a square lattice located in the plane $Z = 0$. Nonadsorbed blocks (blocks B) are described by a three-dimensional self-avoiding walk on a cubic lattice above the surface. This model accounts for the experimental observations that the P2VP blocks are strongly adsorbed on the substrate, so that most monomeric units form trains and the fraction and the length of loops are very small. The number of A block units, N_a, was chosen to be equal to 16 and kept constant for all simulations presented here. The number of B-block segments was varied, $N_b = 4, 8, 16$.

The number of chains in the simulation box was chosen to be $n = 128$, so that the 2D volume fraction of

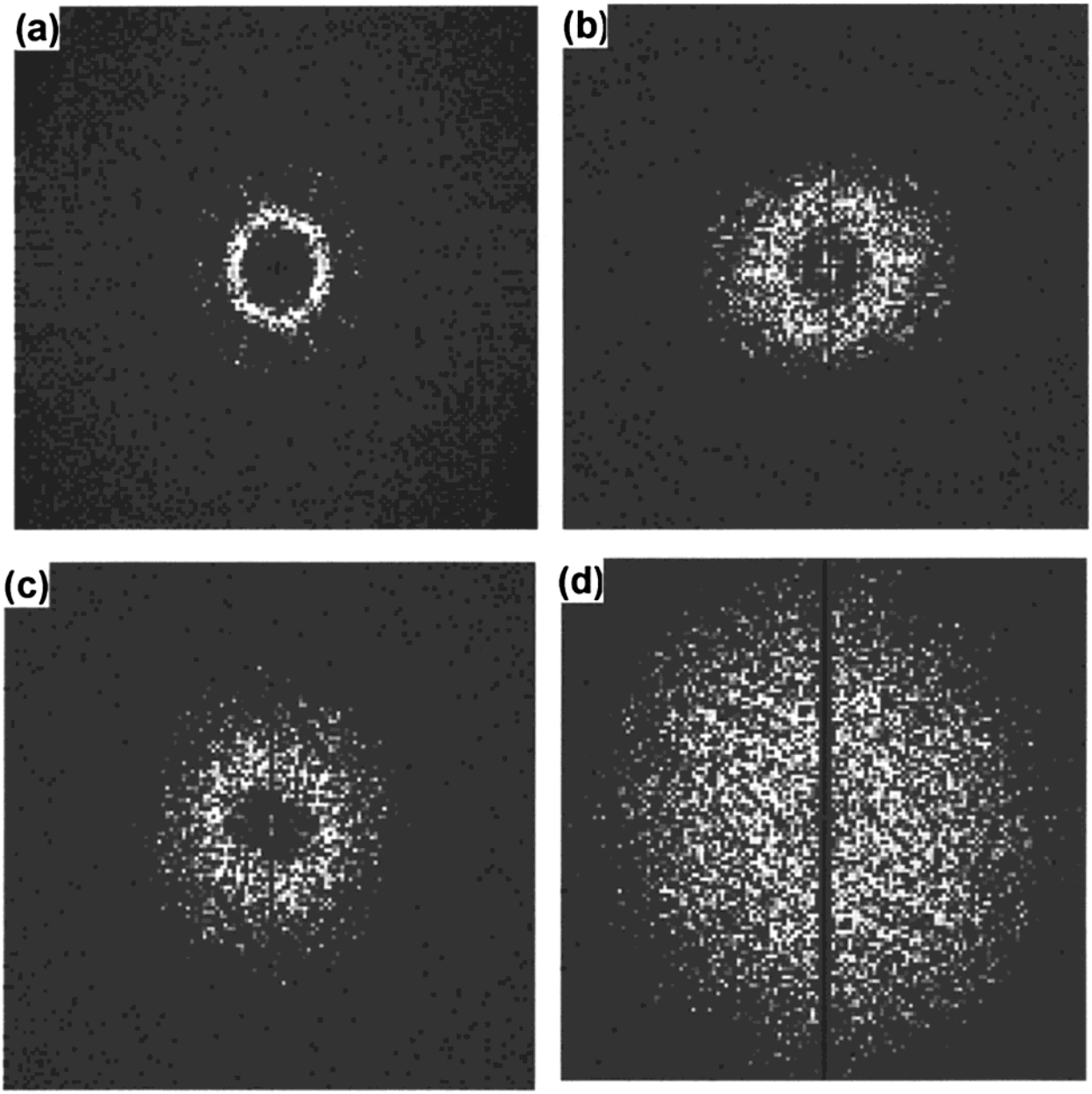

Figure 2. Two-dimensional Fourier transformation of the images shown in Figure 1a−d.

the monomeric units A on the plane $Z = 0$ is $\rho = 4nN_a/L^2$, which roughly corresponds to the case of a two-dimensional melt.

The value of Z_0 was chosen according to the length of B blocks, N_b, always to be larger than the length of fully stretched B blocks. Thus, the B chains could not interact with the Z_0 plane.

In addition to the excluded-volume interactions between all monomeric units, the monomeric units of the B blocks interact via an attractive potential

$$U_c(R_{ij}) = \begin{Bmatrix} -\epsilon, r_{i,j} \le r^* \\ 0, r_{i,j} > r^* \end{Bmatrix} \quad (1)$$

where $r_{i,j}$ is the lattice distance between two monomer units i and j belonging to the same B block or to different B blocks, ϵ is the energy parameter, and $r^* = \sqrt{12}$.

A trial configuration is accepted if it is free of overlap with the transition probability

$$P_{\alpha,\beta} = \min(1, \omega_{\alpha,\beta}) \quad (2)$$

where $\omega_{\alpha,\beta} = \exp[-(U_\alpha - U_\beta)/k_B T]$, $U_\alpha = U_\alpha[\{r_\alpha\}]$ and $U_\beta = U_\beta[\{r_\beta\}]$ being the system potential energies in the configurations $\{\vec{r}_\alpha\}$ and $\{\vec{r}_\beta\}$.

The time, t, is measured in Monte Carlo steps (MCS) per segment. One MC step means that on average each segment has attempted to move once, successfully or unsuccessfully.

Initial configurations of the system were constructed by adding randomly polymer chains into the simulation box (A blocks on the plane $Z = 0$) without overlapping of nonbonded units. Afterward, the system was equilibrated for 500 000 MCS at $\epsilon = 0$.

Only then, the attraction interaction ϵ between b segments was increased gradually. It has to be mentioned that the final state of the system at fixed ϵ depends crucially on the rate of the quenching. For the calculations presented here, we changed the value of ϵ very slowly (with the step 0.01) and equilibrate the system for 500.000 MCS at each value of ϵ.

Snapshot pictures for the systems with $N_b = 4$, 8, 16 and $\epsilon = 0.42$ are shown in Figure 4. One can see that

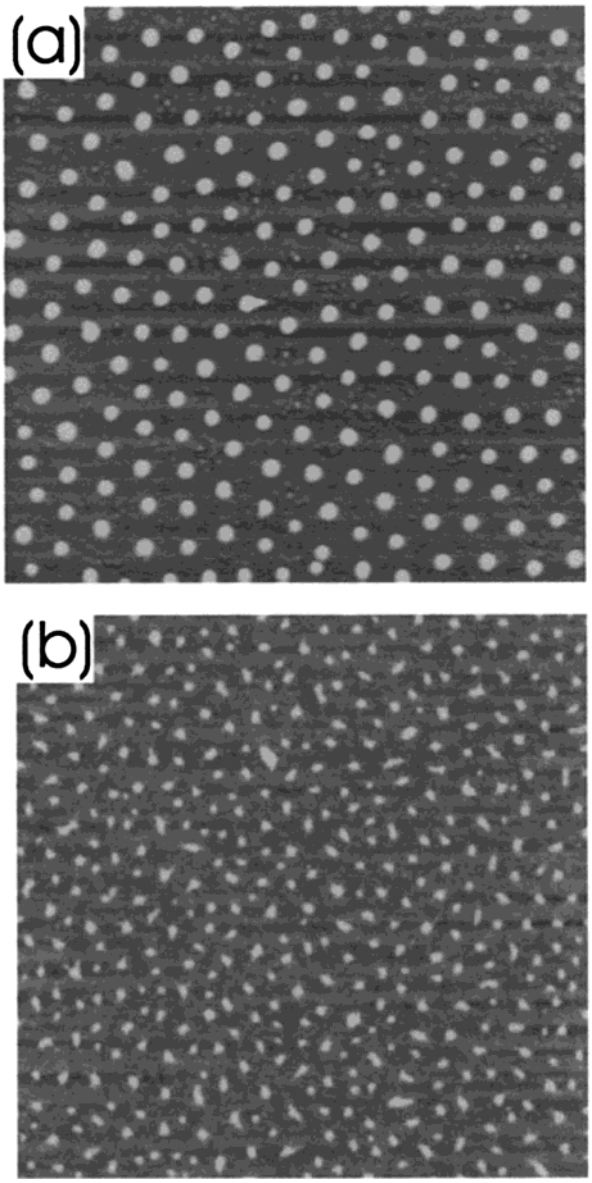

Figure 3. SFM topography images of laterally phase separated PS(1350)-*b*-P2VP(450) diblock copolymer films on (a) mica and (b) GaAs wafer. The gray scale indicates the height values ranging from 0 nm for black and 30 nm for white features. The length of each image corresponds to 5 μm.

the system with $N_b = 16$ has a well-defined micellar structure on the surface. For $N_b = 8$ the distribution of aggregate sizes is very broad, and the number of chains in one micelle is smaller. Finally, for the shortest length of the B block, $N_b = 4$, one cannot distinguish any aggregates, and the distribution of chain segments on the plane is homogeneous.

To characterize the behavior of the system, we calculated the static structure factor

$$S(q) = \frac{1}{n}\sum_{i,j}^{n}\langle e^{i\vec{q}(\vec{r}_i - \vec{r}_j)}\rangle$$

where $\vec{r}_i$ and $\vec{r}_j$ are the position vectors of the ith and the jth junction points between A and B blocks, $\vec{q}$ is the scattering wave vector, and angle brackets stand for the average over all configurations.

Figure 5a shows the static structure factors as functions of the wave vector for the adsorbed block copolymers for $\epsilon = 0.42$ and various values of the length of nonadsorbed B blocks, $N_B = 4$, 8, 16 (corresponding to the systems which snapshots are shown in Figure 4). $S(q)$ for $N_b = 16$ has a well-defined maximum at $q = 0.14$ while the structure factor for the system with $N_b = 4$ is a monotonic function of q. Thus, at the fixed value of $\epsilon = 0.42$ the surface micelles are found in the system

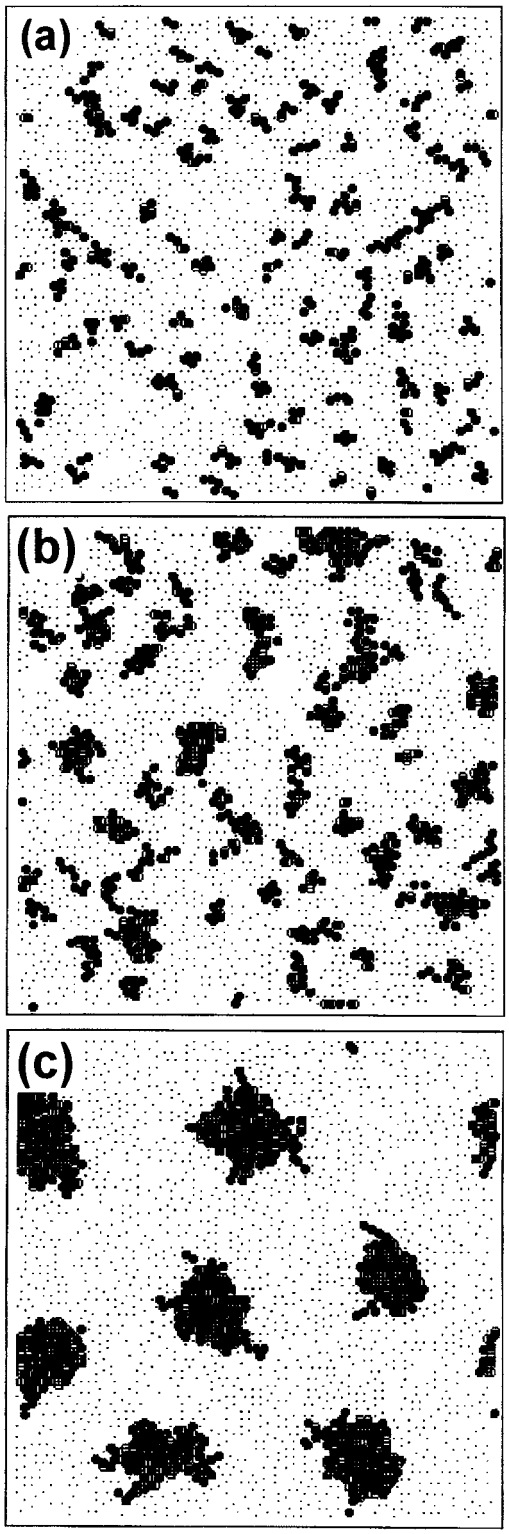

Figure 4. Computer simulation of diblock copolymer adsorption by the Monte Carlo lattice method. The images represent snapshot pictures (top views) for systems with $N_b = 4$, 8, 16 and $\epsilon = 0.42$. Adsorbed A monomer units are shown as gray points, and dark spheres depict monomer units of B type.

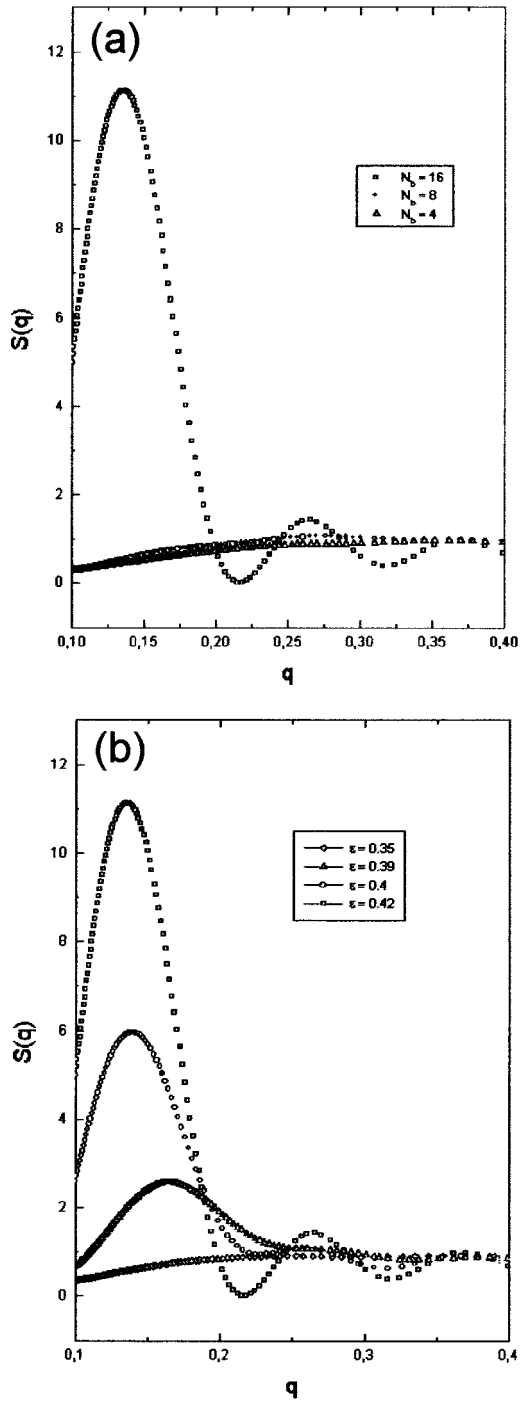

Figure 5. (a) Static structure factors as a function of the wave vector for adsorbed block copolymers with $\epsilon = 0.42$ and various values of the length of nonadsorbed B blocks. (b) Static structure factors as functions of the wave vector for adsorbed block copolymers with $N_a = N_b = 16$ and various values of ϵ.

with longer B blocks while for shorter B blocks the aggregation of B chains in micelles is not observed in accordance with Figure 4. That is, the system becomes more ordered if the length of the nonadsorbed block is increased.

In Figure 5b we present the static structure factor, $S(q)$, as a function of the wave vector $\vec{q}$ for different values of ϵ. For $\epsilon = 0.35$ the function $S(q)$ is monotonic, which corresponds to the homogeneous distribution of the junction points on the plane $Z = 0$ (curve i). For $\epsilon = 0.42$ the dependence $S(q)$ has a peak at $q = 0.14$ (curve iv). The appearance of the peak demonstrates aggregation of the B segments which leads to an inhomogeneous distribution of junction points on the plane $Z = 0$. The value of q at which $S(q)$ has a maximum value, q_m, characterizes the spatial scale of inhomogeneties in the system; i.e., $r = 2\pi/q_m$ is the average distance between aggregates. One can see that with the increase in ϵ the peak in $S(q)$ becomes sharper and shifts to smaller values of q. The system becomes more ordered.

Conclusions

SFM experiments and the Monte Carlo simulation clearly demonstrated that the surface interaction can induce lateral phase segregation in an ultrathin film of a diblock copolymer with one block that interacts strongly with the substrate and a second block whose interaction with the other components is generally unfavorable. Beside the interaction potential, the length of the nonadsorbing block plays a crucial role in the formation of a regular surface pattern. The computer simulations allowed to describe the occurrence of an order-to-disorder transition in good agreement with the experimental observations, yielding a rather remarkable coincidence between the experimental SFM images and the simulation snapshots (see Figure 1 versus Figures 4 and 5a). Correspondingly, also the effect of the interaction potential could be simulated in agreement with the experiments. Figure 5b demonstrates that already relatively small changes in the interaction potential can reduce the order drastically. Experimentally, this was done when a GaAs wafer was used as the substrate instead of mica. Yet it must be noted that the nature of the interaction of the vinylpyridine units with mica and GaAs is not sufficiently understood to rationalize the significant difference. Ionic interactions might play an important role in the case of mica. We can, however, also not exclude kinetic trapping of the surface pattern on the GaAs substrate that might impede equilibration of the structure during annealing.

The results reported here fall in line with a scaling analysis of the surface-induced lateral segregation which demonstrated that the diameter of the surface clusters and the aggregation number scales with the length of B blocks as $N_b^{1/2}$.[10] A comprehensive comparison of the experimental data and the theoretical predictions will be described in a forthcoming report.[23]

Acknowledgment. This work was supported by the Deutsche Forschungsgemeinschaft (Graduiertenkolleg 329). E.Yu.K., I.I.P., and A.R.Kh. are grateful to the Russian Foundation for Basic Research for financial support.

References and Notes

(1) E.g.: Bates, F. S.; Frederickson, G. H. *Annu. Rev. Phys. Chem.* **1990**, *41*, 525.

(2) Krausch, G. *Mater. Res. Rep.* **1995**, *14*, 1.

(3) Amdal, K.; Rosedal, J. H.; Bates, F. S.; Wignall, G. S.; Frederickson, G. H. *Phys. Rev. Lett.* **1990**, *56*, 1112.

(4) Anastasidas, S. H.; Russel, T. P.; Satija, S. K.; Majkrzak, C. F. *J. Chem. Phys.* **1990**, *92*, 5677.

(5) Kellogg, G. J.; Walton, D. G.; Mayes, A. M.; Lambooy, P.; Russell, T. P.; Gallagher, P. D.; Satija, S. K. *Phys. Rev. Lett.* **1996**, *76*, 2503.

(6) Mansky, P.; Liu, Y.; Huang, E.; Russell, T. P.; Hawker, C. J. *Science* **1997**, *275*, 1458.
(7) Mansky, P.; Russell, T. P.; Hawker, C. J.; Mays, J.; Cook, D. C.; Satija, S. K. *Phys. Rev. Lett.* **1997**, *79*, 237.
(8) Morkved, T. L.; Wiltzius, P.; Jaeger, H. M.; Grier, D. G.; Witten, T. A. *Appl. Phys. Lett.* **1994**, *64*, 422.
(9) Morkved, T. L.; Lu, M.; Urbas, A. M.; Ehrichs, E. E.; Jaeger, H.; Mansky, P.; Russell, T. P. *Science* **1996**, *273*, 931.
(10) Harrison, C.; Park, M.; Chaikin, P. M. *Polymer* **1998**, *39*, 2733.
(11) Radzilowski, L. H.; Carvalho, B. L.; Thomas, E. L. *J. Polym. Sci., Part B* **1996**, *34*, 3081.
(12) Spatz, J. P.; Sheiko, S.; Möller, M. *Adv. Mater.* **1996**, *8*, 513.
(13) Spatz, J. P.; Möller, M.; Noeske, M.; Behm, R. J.; Pietralla, M. *Macromolecules* **1997**, *30*, 3874.
(14) Spatz, J. P.; Eibeck, P.; Mössmer, S.; Möller, M.; Herzog, T.; Ziemann, P. *Adv. Mater.* **1998**, *10*, 849.
(15) Kramarenko, E. Y.; Potemkin, I. I.; Khokhlov, A. R.; Winkler, R. G.; Reineker, P. *Macromolecules* **1999**, *32*, 3495.
(16) Potemkin, I. I.; Kramarenko, E. Y.; Khokhlov, A. R.; Winkler, R. G.; Reineker, P.; Eibeck, P.; Spatz, J. P.; Möller, M. *Langmuir* **1999**, *15*, 7290.
(17) Zhu, J.; Eisenberg, A.; Lennox, R. B. *Langmuir* **1991**, *7*, 1579.
(18) Kuamaki, J.; Hashimoto, T. *J. Am. Chem. Soc.* **1998**, *120*, 423.
(19) Künstle, H. Block Copolmer Composites With Semiconductor Nanocrystals. Ph.D. Thesis, Holland, 1993.
(20) Spatz, J. P.; Mössmer, S.; Hartmann, Ch.; Möller, M.; Herzog, T.; Krieger, M.; Boyen, H.-G.; Ziemann, P. *Langmuir*, in press.
(21) Carmesin, I.; Kremer, K. *Macromolecules* **1988**, *21*, 2819.
(22) Deutsch, H.-P.; Binder, K. *J. Chem. Phys.*, **1991**, *94*, 2294.
(23) Eibeck, P.; Spatz, J. P.; Mössmer, S.; Möller, M.; Potemkin, I. I.; Kramarenko, E. Y.; Khokhlov, A. R.; Winkler, R. G.; Reineker, P., to be submitted.

MA990751P